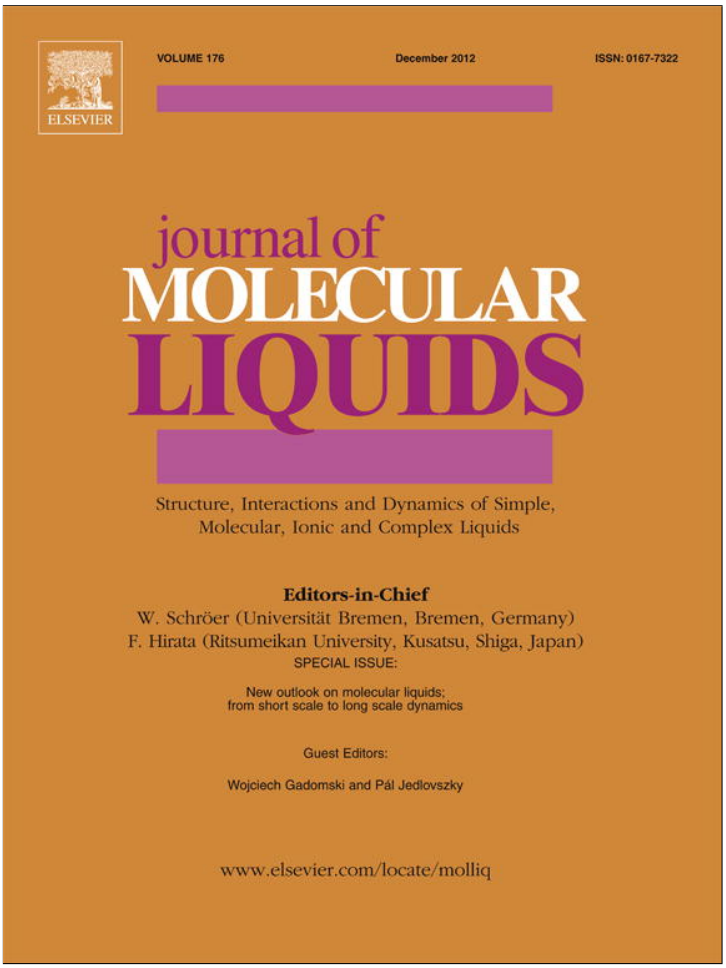

Journal of Molecular Liquids 176 (2012) 60–64

Contents lists available at SciVerse ScienceDirect

Journal of Molecular Liquids

journal homepage: www.elsevier.com/locate/molliq

Light scattering study of human serum albumin in pre-denaturation: Relation to dynamic transition in water at 42 °C

Vitaliy Bardik [a,*], Vladimir Gotsulskii [b], Evgen Pavlov [c], Nikolai Malomuzh [b], Dmitry Nerukh [c], Igor Yanchuk [d], Serhiy Lavoryk [d]

[a] Kiev National Taras Shevchenko University, Physics Faculty, Prospect Acad. Glushkova, 4, Kiev 03127, Ukraine
[b] Odessa Mechnikov National University, Dvoryanskaya str., 2, Odessa 65026, Ukraine
[c] Aston University, Non-linearity and Complexity Research Group, Birmingham, B4 7ET, UK
[d] Nanomedtech, Gor'kogo str., 68, Kiev 03150, Ukraine

ARTICLE INFO

Available online 26 September 2012

Keywords:
Dynamic light scattering
Conformational dynamics
Human serum albumin
Hydrogen bonds
Hydrodynamic radius

ABSTRACT

Protein functional motions are ultimately connected to water dynamics. The goal of this study is to link the conformational dynamics of albumin to a dynamic transition taking place at ~42 °C in water. We report the results of dynamic light scattering measurements of albumin aqueous solution in the temperature interval 20–65 °C. The processing of the experimental data produced the temperature dependence of the macromolecular hydrodynamic radius. We demonstrate that the growth of the macromolecular size in this temperature range can be divided into two stages that are connected to the dynamical properties of water.

1. Introduction and background

Protein conformation and its dynamics define protein's biological functioning. Despite very intensive research the molecular mechanisms and the driving forces of conformational changes are largely unknown. What is generally accepted is the key role of water in protein conformational dynamics.

Frauenfelder and colleagues have experimentally shown that protein dominant conformational motions are slaved by the hydration shell and the bulk solvent [1], while the protein molecule itself provides an 'active matrix' necessary for guiding the water dynamics towards the biologically relevant conformational changes (the protein's 'function' or folding). The change in water dynamics at the shell of up to 20 Å (almost a dozen water molecule diameters) around proteins has been demonstrated in the work [2]. Many other experimental and simulation works support the fact of ultimate connection between liquid water dynamical properties and protein unique conformational motions [3–6]. The specific property of water and other glass-forming liquids responsible for this behavior is their 'dynamic heterogeneity' manifested in the long known, but still poorly understood α- and β-relaxation phenomena in liquid and supercooled water [7,8]. The essence of the phenomenon is the existence of spatially separated areas in the liquid with qualitatively different dynamical properties dictated by collective intermolecular interactions and in the case of water by the peculiarities of the hydrogen bonding network.

In comparison with the majority of one component liquids water shows many unusual properties which were the subject of extensive studies for many years [9,10]. It was shown in [11], by separating the contributions of different physical nature, that the behavior of the normalized shear viscosities for water and argon can be compared using the corresponding states principle. The analysis of the temperature dependences of the reduced shear viscosity of water and argon has revealed the temperature point $T_H = 42$ °C, from which the behavior of these substances becomes similar (Fig. 1). The kinematic shear viscosity of liquids is one of the main transport coefficients. It is formed by different components of the thermal motion of molecules, in the first place, by the translational and rotational degrees of freedom. For water the significant influence on the manifestation of its properties is produced by hydrogen (H) bonds. Thus, if a molecule is connected with its nearest neighbors by three or four H-bonds, it can only oscillate around some temporary equilibrium position.

Analogous results have been obtained on the basis of the temperature dependencies analysis of the normalized fraction of volume and the normalized heat of evaporation for water and argon (Figs. 2 and 3) [12].

For the molecular interpretation of these data it was proposed that the molecular motion below T_H has a crystal like character. The descriptive criterion for this region is the validity of the strong inequality $\tilde{\tau} = \frac{\tau_0}{\tau_1} >> 1$, where τ_0 is the residence time or the time of small

* Corresponding author.
E-mail address: vital@univ.kiev.ua (V. Bardik).

0167-7322/$ – see front matter © 2012 Elsevier B.V. All rights reserved.
http://dx.doi.org/10.1016/j.molliq.2012.09.012

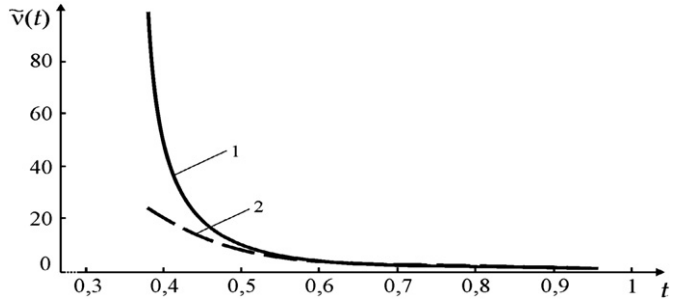

Fig. 1. Temperature dependence of the reduced viscosity of water (1) and argon (2), temperature is in reduced units, $T_H \approx 0.55$ (taken from [11]).

oscillations of a molecule near its temporary equilibrium position [13], τ_1 is the time of transition to another temporary equilibrium position: $\tau_1 \approx \frac{1}{\sqrt{1/kT}} \approx 5 \cdot 10^{-13} s$. This situation is illustrated schematically in Fig. 4. Thus, the derivation of the temperature dependence of $\tilde{\tau}$ allows to establish the region of the crystal like representation of water. The detailed analysis of $\tilde{\tau}$ as a temperature function has been carried out on the basis of the quasi-elastic incoherent neutron scattering data in [14,15].

In the vicinity of T_H the ratio of the characteristic times tends to 1. We, therefore, suggest that the character of the thermal motion in water at $T_H = (315 \pm 3)$ K undergoes a especial transformation, which will be qualified by us as a dynamic transition. The rapid growth of the residence time τ_0 with the temperature decay can be naturally interpreted

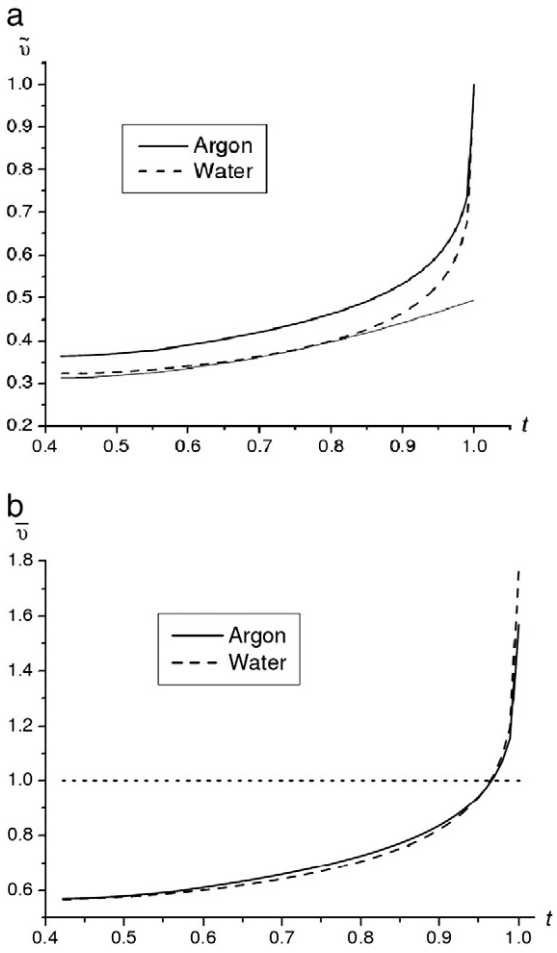

Fig. 2. Temperature dependencies of the normalized fraction volume for water and argon: a) $\tilde{\upsilon}(t) = \upsilon(t)/\upsilon_c$, b) $\bar{\upsilon}(t) = \upsilon(t)/\upsilon_R$. The light line in a) corresponds to $0.86 \cdot \tilde{\upsilon}_R^{(Ar)}(t)$ (taken from [12]).

in the framework of cluster representations, especially characteristic for supercooled states. Indeed, it had been shown in [16] that the relative volume occupied by the crystal like clusters increases from the value $\varphi = 0.11$ at the melting temperature $T_m = 273$ K up to $\varphi = 0.41$ at $T = 243$ *K*. For these states of water τ_0 can be identified as the lifetime of the crystal like clusters. Their average size changes more slowly and remains close to 10 Å. Note that among clusters, the leading role belongs to the hexagonal rings, which are the building elements for the ordinary (hexagonal) ice. Probably, $\varphi \to 0$ when $T \to T_H$. The crystal like picture of the thermal motion in water near the melting point is also supported by the results of computer simulations presented in [17]. There it was shown that for $T < 284$ K the increment of the mean square displacement of a molecule is close to zero in the time interval 10^{-13} s$< \tau_0$, where $\tau_0 > 10^{-12}$ s starting from $T \leq T_m$.

These data testify that the global hydrogen bonding network disintegrates into an ensemble of weakly interacting clusters: dimers, trimers, tetramers, etc. [15]. In other words, the spatial connectivity between linear molecular chains is disrupted in the vicinity of $T \approx T_H$. All these facts lead to the conclusion that the temperature of 42 °C is the point of a *dynamic transition* in water.

The value of T_H coincides with the physiological temperature at which the thermal denaturation of proteins takes place. As denaturation (unfolding) is a form of conformational dynamics of proteins, the dynamic transition can have an effect on the protein's elementary conformational changes.

The goal of the article is to relate the conformational dynamics of proteins at the level of macromolecular size to the dynamic properties of water (within the framework of the 42 °C hypothesis describing the transition when the 'liquid like' molecular motion changes to the 'gas like' one) in the temperature range 25 °C–60 °C, especially in the vicinity of $T_H \approx 42$ °C as the threshold temperature of protein conformational stability.

Here we report the results of studying aqueous human serum albumin solution (HSA). HSA is a single chain protein with 585 amino acids, with a molecular weight of ~67,000 Da. The structure of this protein has been determined by X-ray crystallography of high resolution [18]. HSA plays a special role in transporting metabolites and drugs throughout the vascular system and also in maintaining the pH and osmotic pressure of plasma [19]. HSA structure and dynamics are known to be influenced by several factors, like pH, temperature, and binding of different ligands [20]. There is a number of investigations of HSA by fluorescent [21], IR [22], and NMR spectroscopies [23]. However, to the best of our knowledge, there are no studies of the connection between the size and structure of the protein molecule and its hydration, especially at different temperatures.

2. Methodology, results, and discussion

Aqueous solution of HSA at concentrations 1 wt.% with ions K^+ and Na^+ 5 mmol/l was investigated by dynamic light scattering technique (DLS), also known as photon correlation spectroscopy (PCS) [24]. This technique has been successfully applied in studies of growth of fractal aggregates in water solutions of albumin and DNA [25], aqueous solutions of poly(ethylene glycol) [26], diffusive processes of alcohols and semidilute polymer solutions [27–29], cluster growth in aqueous sugars and glass-forming aqueous glucose solutions [30,31]. The measurements have been performed in the temperature interval 25 °C–50 °C with the 1 °C step. The vertically polarized light 632.8 nm from a helium-neon laser was focussed onto the sample (the beam diameter in the scattering volume 0.3 mm, scattering is regulated by the vertical slit diaphragm) and the light scattered at 45° was recorded by a photomultiplier. The diaphragm restricting the aperture of a scattering beam was located before photocathode. The homodyne detection was used in our study. The photoimpacts were digitized and fed to a correlator which computed intensity–intensity correlation function, which, for monodisperse samples consisting of a single particle size

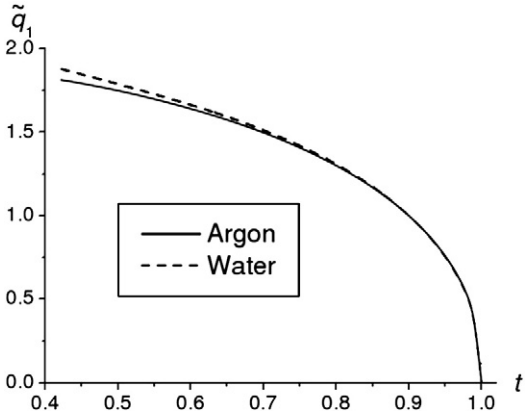

Fig. 3. Temperature dependencies of the normalized heat of evaporation $\tilde{q}$ for water and argon, where $\tilde{q} = \frac{q}{q_0}$, where q_0 is the heat of evaporation at $t = 0.9$ (taken from [12]).

group, can be fit to a single exponential form as given in the following expression

$$G^{(2)}(\tau) = B + AG^{(1)}(\tau), \tag{1}$$

where, $G^{(1)}(\tau) = \exp\{-2q^2D\tau\}$ — first order correlation function, $q = \frac{4\pi n}{\lambda}\sin(\frac{\theta}{2})$, B is the baseline, A is a constant depending on spatial coherence, and D is the diffusion coefficient, λ is the vacuum wavelength of the laser, and θ is the scattering angle. Correlation is a second order statistical technique for measuring the degree of non-randomness in an apparently random data set. When applied to a time dependent intensity trace, as measured by a DLS instrument, the correlation coefficient is the intensity-intensity autocorrelation function calculated as

$$G^{(2)}(\tau) = \int_0^\infty I(t)I(t+\tau)dt \tag{2}$$

or

$$G^{(2)}(\tau) = \frac{\langle I(0)I(\tau)\rangle}{I^2}, \tag{3}$$

where τ is the delay time. Typically, the autocorrelation function is normalised, such that $G(\infty) = 1$. For the monochromatic laser light this normalization imposes an upper correlation limit of 2 for $G(\tau_0)$ and a lower baseline limit of 1 for $G(\infty)$. In practice, experimental upper limits for a DLS correlogram are typically around 1.8 to 1.9. In DLS, all information regarding the motion or diffusion of the particles in the solution is embodied within the measured correlation curve [24].

As a result we have obtained the autocorrelation function (1) processed by the described regularization methods at different temperatures (Fig. 5). Processing these data provided the temperatures dependences of the macromolecule hydrodynamic radius (Fig. 6) calculated using the particle diffusion coefficient obtained from Eq. (1) and the Stokes–Einstein equation

$$R_H = \frac{kT}{6\pi\eta D}, \tag{4}$$

where k is the Boltzmann constant, T is the temperature, and η is the dispersant viscosity.

Another set of measurements has been carried out using commercial spectrometer Zetasizer Nano ZS (ZEN3600). This technique processes the data using the cumulant analysis [32]. The cumulant analysis is essentially the fit of a polynomial to the log of the $G^{(1)}(\tau)$ correlation function

$$\ln\left(G^{(1)}(\tau)\right) = a + b\tau + c\tau^2 + d\tau^3 + \ldots \tag{5}$$

The value of b is known as the second order cumulant, or the Z-average diffusion coefficient. This is converted to the size using the dispersant viscosity and some instrumental constants. Only the first three terms a, b, and c are used in the standard analysis to avoid overresolving the data; however this does mean that the Z-average size is likely to be interpreted incorrectly if the distribution is very broad (i.e. has a high polydispersity).

The cumulant analysis gives a good description of the size that is comparable with other methods for spherical, reasonably narrow monomodal samples, i.e. with polydispersity below the value of 0.1. For samples with a slightly increased width, the Z-average size and polydispersity gives values that can be used for comparative purposes. For broader distributions, where the polydispersity is over 0.5, it is unwise to rely on the Z-average mean, and a distribution analysis should be used to determine the peak positions. The values of the hydrodynamic radii obtained from the Z-average diffusion coefficient (formula (5)) in the temperature interval 20 °C–70 °C are presented in Fig. 7.

Based on the obtained data we conclude that the change of the macromolecular hydrodynamic radius with temperature is a two-stage process. The first stage is the increase of the radius up to the temperature of dynamic transition in water at $T_H \approx 42$ °C. The second stage is the increase of its value up to the denaturation temperature. These stages are separated by a 'plateau' in the vicinity of the temperature point T_H, the temperature interval where R_H has a constant value is approximately 3 °C–5 °C. Partly, these results coincide with the data presented in [33] where it was shown that the conformational changes of HSA in the temperature interval 25 °C–55 °C is a process subdivided into three sub-transitions

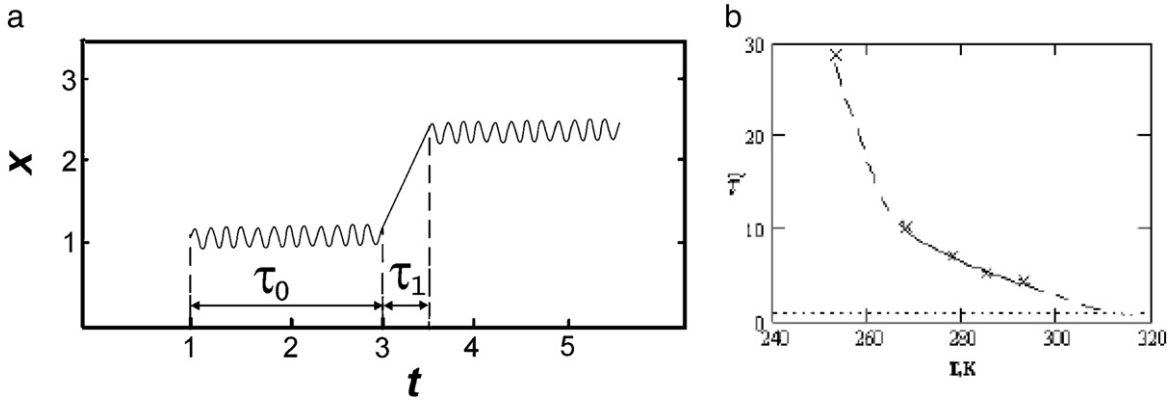

Fig. 4. a) The crystal-like character of the thermal motion in water; b) the temperature dependence of the characteristic times $\tilde{\tau} = \frac{\tau_0}{\tau_1}$ (taken from [14]).

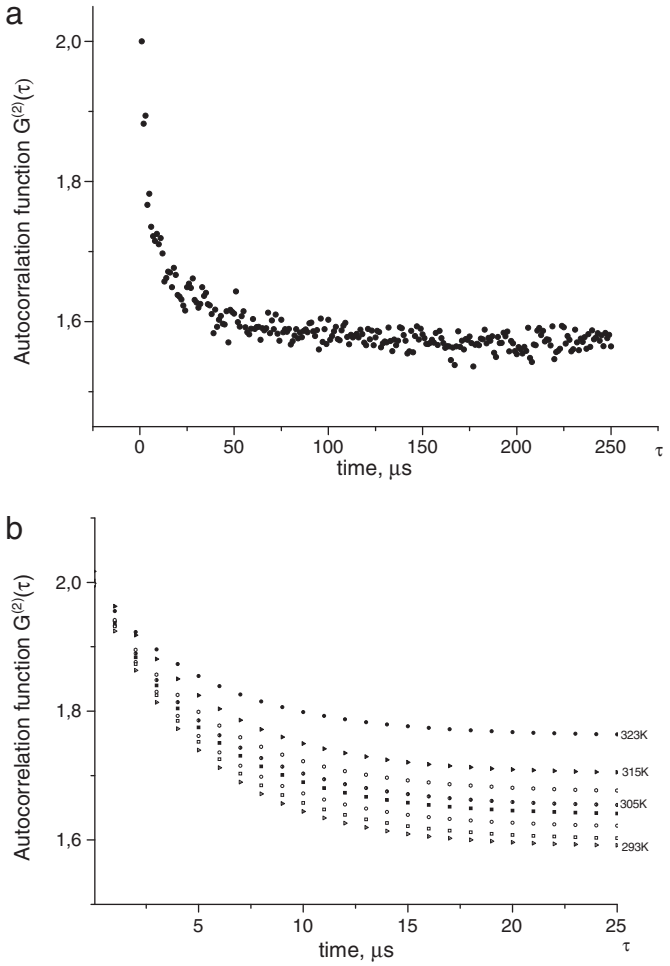

Fig. 5. The time dependence of intensity autocorrelation function $G^2(\tau)$: the experimentally measured $G^{(2)}(\tau)$ (unprocessed data), time step is 10 μs; b) the results of fitting of the experimental data using formula (1) at different temperatures.

which might be related to the links between the three structured domains of HSA. Authors have shown that these sub-transitions are sequential and separated by a temperature interval of approximately 9 °C. Interestingly, the temperature of the last sub-transition coincides with T_H, which is also the maximal value of fever in human body at pathological conditions.

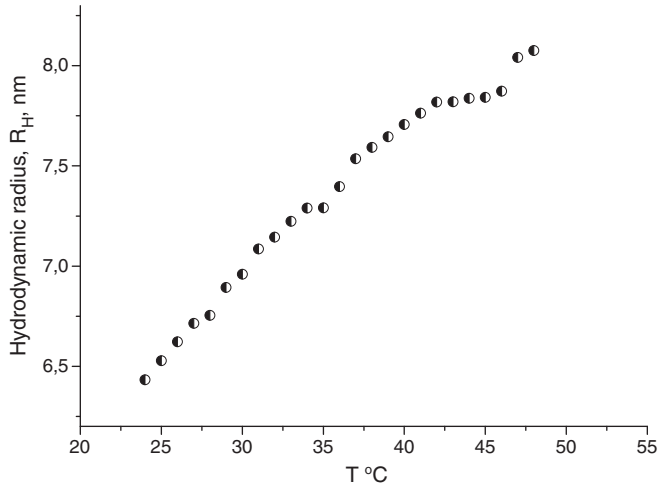

Fig. 6. The temperature dependence of the hydrodynamic radius of albumin macromolecule.

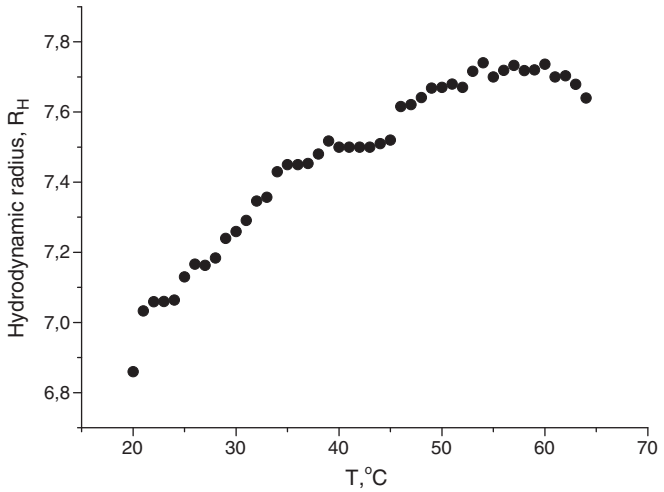

Fig. 7. The values of the hydrodynamic radius in the temperature interval 20 °C–65 °C obtained on Zetasizer.

3. Conclusions

Using the DLS technique we have investigated the temperature dependence of the hydrodynamic radius of albumin in aqueous solution. We have found that the radius increase roughly linearly up to approximately 4025 °C. It then exhibits a 'plateau' in the range ≈40–45 °C. The further increase of the radius follows by a maximum at approximately 55 °C.

We can, thus, hypothesize that the increase of the hydrodynamic radius at the first stage (before the 'plateau') is provided by the swelling of the protein itself. In the interval 40–45 °C the destruction of the hydration shell compensates the increase of the protein core. The second stage related to irreversible conformational changes following protein denaturation.

References

[1] H. Frauenfelder, G. Chen, J. Berendzen, P.W. Fenimore, H. Jansson, B.H. McMahon, I.R. Stroe, J. Swenson, R.D. Young, PNAS 106 (13) (2009) 512.
[2] S. Ebbinghaus, S.J. Kim, M. Heyden, X. Yu, U. Heugen, M. Gruebele, D.M. Leitner, M. Havenith, PNAS 104 (52) (2007) 20749.
[3] B. Born, H. Weingartner, E. Brundermann, M. Havenith, Journal of the American Chemical Society 131 (10) (2009) 3752.
[4] S.E. Pagnotta, S. Cerveny, A. Alegria, J. Colmenero, Physical Chemistry Chemical Physics 12 (35) (2010) 10512.
[5] Q. Johnson, U. Doshi, T. Shen, D. Hamelberg, Journal of Chemical Theory and Computation 6 (9) (2010) 2591.
[6] L. Zhang, Y. Yang, Y.-T. Kao, L. Wang, D. Zhong, Journal of the American Chemical Society 131 (30) (2009) 10677.
[7] V. Lubchenko, P.G. Wolynes, H. Frauenfelder, The Journal of Physical Chemistry. B 109 (15) (2005) 7488.
[8] H.E. Stanley, P. Kumar, S. Han, M.G. Mazza, K. Stokely, S.V. Buldyrev, G. Franzese, F. Mallamace, L. Xu, Journal of Physics: Condensed Matter 21 (50) (2009) 504105.
[9] G. Robinson, S.-B. Zhu, S. Singh, M.W. Evans, Water in biology, chemistry and physics. Experimental overviews and computationnal methodologies, World Scientific Publishing, Singapore, 1996.
[10] D. Eisenberg, W. Kauzmann, The Structure and Properties of Water, 1st Edition Oxford University Press, New York, 1969.
[11] L.A. Bulavin, A.I. Fisenko, N.P. Malomuzh, Chemical Physics Letters 453 (2008) 183.
[12] A.I. Fisenko, N.P. Malomuzh, A.V. Oleynik, Chemical Physics Letters 450 (2008) 297.
[13] K. Singwi, A. Sjolander, Physical Review 119 (1960) 863–871.
[14] A.I. Fisenko, N.P. Malomuzh, International Journal of Molecular Sciences 10 (2009) 2383–2411.
[15] T.V. Lokotosh, N.P. Malomuzh, K.N. Pankratov, Journal of Chemical & Engineering Data 55 (2021) (2010).
[16] T.V. Lokotosh, S. Magazu, G. Maisano, N.P. Malomuzh, Physical Review E 62 (2000) 3572.
[17] P. Gallo, F. Sciortino, P. Tartaglia, S.H. Chen, Physical Review Letters 76 (1996) 2730.
[18] S. Sugio, A. Kashima, S. Mochizuki, M. Noda, K. Kobayashi, Protein Engineering 12 (1999) 439.

[19] M. Ikeguchi, S. Sugai, M. Fujino, T. Sugawara, K. Kuwajima, Biochemistry 31 (1992) 12695.
[20] J.R. Brown, in: V.M. Rosenoer, M. Oratz, M.A. Rothschild (Eds.), Albumin structure, function and uses, Pergamon Press, Oxford, UK, 1977.
[21] Y. Marechal, Journal of Molecular Structure 700 (SI) (2004) 217.
[22] V.V. Kuvichkin, V.V. Novikov, F.K. Alyushev, et al., Biofizika 46 (2001) 43.
[23] V.V. Turov, V.A. Pokrovsky, A.A. Chujoko, Biofizika 39 (1994) 988.
[24] H.Z. Cummins, E.R. Pike, Photon correlation and light beating spectroscopy, Plenum press, New York and London, 1974. Published in cooperation with NATO Scientific Affairs Division.
[25] S. Magazu, G. Maisano, F. Mallamace, N. Micali, Physical Review A 39 (1989) 4195.
[26] D.I. Donato, M.P. Janelli, S. Magazu, G. Maisano, D. Majolino, P. Migliardo, R. Ponterio, Journal of Molecular Structure 381 (1996) 213.
[27] M.P. Jannelli, S. Magazu, P. Migliardo, U. Wanderlingh, Physica B: Condensed Matter 234 (1997) 355.
[28] M.P. Jannelli, S. Magazu, P. Migliardo, F. Aliotta, E. Tettamanti, Journal of Physics: Condensed Matter 8 (1996) 8157.
[29] A. Faraone, S. Magazu, G. Maisano, R. Ponterio, V. Villari, Macromolecules 32 (1999) 1128.
[30] D.L. Sidebottom, Physical Review E 76 (011505) (2007).
[31] D.L. Sidebottom, Tri D. Tran, Physical Review E 82 (2010) 051904.
[32] D.E. Koppel, Journal of Chemical Physics 57 (1972) 4814.
[33] M. Rezaei-Tavirani, S.H. Moghaddamnia, B. Ranjbar, M. Amani, S.A. Marashi, Journal of Biochemistry and Molecular Biology 39 (5) (2006) 530–536.